Bioorganic & Medicinal Chemistry Letters 22 (2012) 6205–6211

Contents lists available at SciVerse ScienceDirect

Bioorganic & Medicinal Chemistry Letters

journal homepage: www.elsevier.com/locate/bmcl

Potent and orally efficacious benzothiazole amides as TRPV1 antagonists

Yevgeni Besidski [a], William Brown [b], Johan Bylund [a], Michael Dabrowski [a], Sophie Dautrey [b], Magali Harter [b], Lucy Horoszok [a], Yin Hu [a], Dean Johnson [b], Shawn Johnstone [b], Paul Jones [b], Sandrine Leclerc [b], Karin Kolmodin [a], Inger Kers [a], Maryse Labarre [b], Denis Labrecque [b], Jennifer Laird [b], Therese Lundström [a], John Martino [b], Mickaël Maudet [b], Alexander Munro [b], Martin Nylöf [a], Andrea Penwell [b], Didier Rotticci [a], Andis Slaitas [a], Anna Sundgren-Andersson [a], Mats Svensson [a], Gitte Terp [a], Huascar Villanueva [a], Christopher Walpole [b], Ronald Zemribo [a], Andrew M. Griffin [b,*]

[a] AstraZeneca R&D Södertälje, S-151 85 Södertälje, Sweden
[b] AstraZeneca R&D Montréal, 7171 Frédérick-Banting, St. Laurent, Québec H4S 1Z9, Canada

ARTICLE INFO

Article history:
Received 12 June 2012
Revised 23 July 2012
Accepted 1 August 2012
Available online 14 August 2012

Keywords:
TRPV1 antagonist
Benzothiazoles
Metabolic stability
In vivo pain models

ABSTRACT

Benzothiazole amides were identified as TRPV1 antagonists from high throughput screening using recombinant human TRPV1 receptor and structure–activity relationships were explored to pinpoint key pharmacophore interactions. By increasing aqueous solubility, through the attachment of polar groups to the benzothiazole core, and enhancing metabolic stability, by blocking metabolic sites, the drug-like properties and pharmokinetic profiles of benzothiazole compounds were sufficiently optimized such that their therapeutic potential could be verified in rat pharmacological models of pain.

The transient receptor potential cation channel subfamily V member 1 (TRPV1), also known as VR1, is a member of the transient receptor potential family of ion channels and is a non-selective cation channel with high permeability to divalent cations, especially calcium.[1] It is expressed on unmyelinated pain-sensing nerve fibres and is activated by noxious stimuli, such as heat (>43 °C),[2] low pH,[3] capsaicin **1**[4] (the active component of chili peppers), capsaicin analogues and endocannabinoids.[5] Additionally, prostaglandins and bradykinin modulate TRPV1 through PKC-mediated receptor phosphorylation.[6] Once activated, the channel opens to allow the influx of calcium ions, which in turn leads to the excitation of primary sensory neurons that gate nociceptive inputs to the central nervous system. Studies with TRPV1 knockout mice further substantiate the role that TRPV1 plays in the signaling of pain stimuli.[7] Thus, TRPV1 is an integrator of pain stimuli, and the modulation of TRPV1 therefore represents a potential therapeutic application for the treatment of pain.

Initially, strategies to modulate TRPV1 focused on the development of agonists, since the administration of agonists, such as capsaicin **1**, leads to desensitization of the channel and neurite retraction. However, antagonists at TRPV1, such as capsazepine **2**,[8] (Fig. 1) may prove more useful, since antagonists are devoid of the concomitant pungency and neurotoxicity associated with the administration of agonists.[9]

Benzothiazole **3** (Fig. 2) was identified from a high throughput screening (HTS) campaign using a fluorescence cell-based assay that measures Ca^{2+} influx.[10a] Compound **3** is a potent and competitive antagonist with capsaicin at the TRPV1 receptor, with an IC_{50} of 27 nM. Liabilities of Compound **3** included low aqueous solubility (2.2 μM at pH 7.4) and poor metabolic stability in human microsomes due to oxidation of the *t*butyl and benzylic methyl positions. Our strategy to address these issues included replacing the lypophilic *t*butyl group, reducing lypophilicity through replacement of the right hand aromatic ring with heterocycles, addition of functional groups at the benzylic methyl position and investigating changes to the central amide linker (Fig. 2). It is of interest to note that in addition to our group,[10a] others groups have reported[10b–d] use of the benzothiazole scaffold in their VR1 antagonist programs.

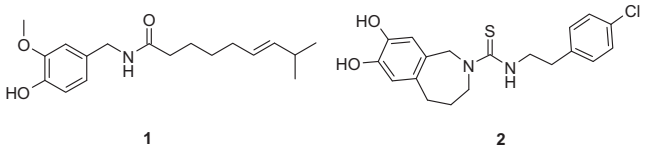

1 2

Figure 1. Structures of TRPV1 antagonists **1** and **2**.

* Corresponding author. Tel.: +1 514 832 3200; fax: +1 514 832 3232.
E-mail address: andrew.griffin@astrazeneca.com (A.M. Griffin).

0960-894X/$ - see front matter © 2012 Elsevier Ltd. All rights reserved.
http://dx.doi.org/10.1016/j.bmcl.2012.08.018

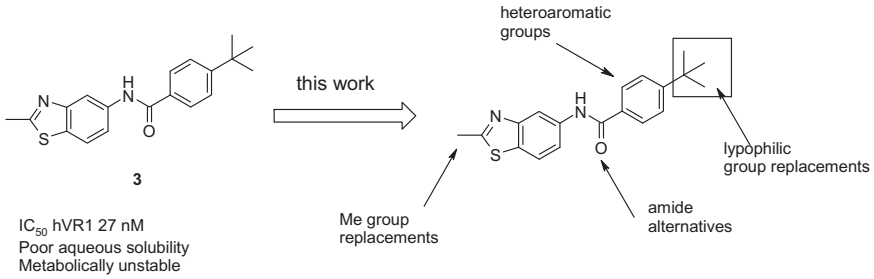

Figure 2. Strategy adopted for optimization of HTS hit **3**.

Metabolism studies showed that the methyl group of benzimidazole **3** was readily oxidized to the corresponding alcohol in vitro. Given that we were looking for improvements in aqueous solubility as well as maintaining TRPV1 activity, we started our SAR exploration by investigating the properties of a set of hydroxymethylbenzimidazoles. Synthesis of hydroxymethylbenzothiazole derivatives was performed using chemistry shown in Scheme 1. Commercially available 2-methyl-1,3-benzothiazol-5-amine was protected as a N-*t*butyl carbamate and the methyl group oxidized with selenium dioxide. The intermediate aldehyde was reduced with sodium borohydride and the alcohol protected as the corresponding allylcarbonate (Alloc). Removal of the Boc protecting group gave aniline **4** which was then followed by amide formation under standard conditions with subsequent removal of the Alloc protecting group to generate alcohols **5**-**21**.

Alternative functional groups were incorporated at the benzylic position and compound **3** served as the starting material for the syntheses of amino-derived analogs **22**–**24** (see Scheme 2). Compound **3** was converted into amine **22** through a three step sequence of oxidation to the corresponding benzylic aldehyde, followed by oxime formation and finally oxime reduction. The amino-derivative **22** was then sulfonylated and acetylated to yield derivatives **23** and **24**, respectively. Synthesis of secondary alcohol **25** was realized by oxidation of **3** to the corresponding aldehyde, followed by addition of methyl magnesium bromide.

Human VR1 antagonism data, as well as aqueous solubility and human microsomal stability data (where available) for alcohols **5**-**21** is shown in Table 1. Alcohol **5**, formed as a metabolite of **3**, maintained excellent potency at VR1 with reasonable metabolic stability. The *t*butyl benzamide group present in **3** and **5** was metabolically labile and efforts were made to examine alternative aromatic amides with various substitution patterns. Replacing the *t*butyl group by a halogen atom usually caused a 10-20 fold loss of potency, although the chloro **6** showed improved metabolic stability. Alternative lypophilic groups such as a trifluoromethyl **9** and alkyl ethers **11** and **12** also showed reasonable activity with moderate solubility, with the para position being preferred for activity (compare para O*t*butyl ether **11** to meta O*t*butyl ether **13**). Efforts to add polar groups in place of the lypophilic groups described so far proved not to be fruitful, such changes being associated with an important loss in potency. Incorporation of a basic nitrogen on the benzamide aromatic ring abolished all activity (compounds **14** and **15**), whereas ethers were tolerated but showed only modest solubility (compounds **16** and **17**). Finally we investigated the use of heterocycles in place of the right hand aromatic group and found this change caused a substantial drop in activity – compare phenyl **9** to pyridyl **18** and pyrrazole **21**. Potency could be regained via addition of a more lypophilic substituent onto the heterocycle (compounds **19**, **20**) but the overall profiles in terms of potency, solubility and metabolic stability did not show significant improvements compared to aromatic derivatives (see Table 1).

Overall, in most cases potency at VR1 was improved switching from the benzylic methyl to hydroxyl methyl substitution as well as demonstrating an improvement in aqueous solubility. These trends were confirmed when looking at a wider set of compounds as shown by a matched pairs analysis (see Fig. 3). A clear need for a lypophilic substituent on the right hand side of the molecule was also confirmed.

Alternative replacements of the alcohol functionality demonstrated a large loss in TRPV1 activity (see Table 2). Amine-derived analogs **22**-**24** showed at least a hundred fold lose of affinity, with sulphonamide **23**, a typical alcohol bioisostere, the most active analog. Secondary alcohol **25**, a racemic compound, showed a 60 fold loss in potency compared to **5**. None of these modifications were pursued further.

Next our attention turned to examining the role of the central amide linker. Reverse amides were synthesized according to Scheme 3. 2-Methyl-1,3-benzothiazol-5-amine was converted to the corresponding aryl iodide via diazotation, and then transformed into cyanide **26** with zinc cyanide under palladium catalysis. The cyano-intermediate was hydrolyzed to acid **27** followed by oxidation of the methyl group according to the same 2-step oxidation/reduction sequence used previously, yielding hydroxy acid **28**. Coupling of acid **28** with 4-*t*-butylaniline furnished **29** while coupling with 4-methyl phenethylamine gave amide **30**.

Sulfonamide **31** was prepared by reacting the corresponding sulfonyl chloride with aminobenzothiazole intermediate **4**, followed by hydrolysis of the allylcarbonate protecting group under

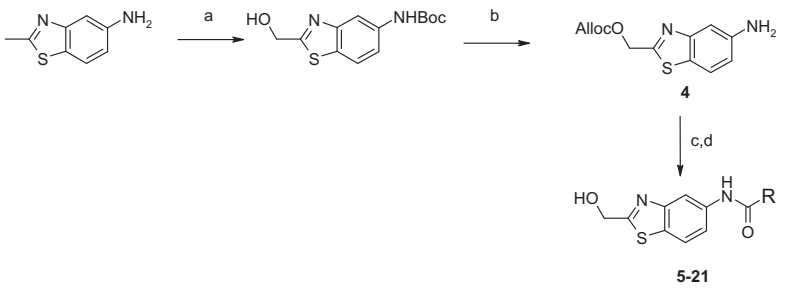

Scheme 1. *Reagents and conditions:*(a) i) Boc_2O, Et_3N, MeOH, 56%; ii) SeO_2, dioxane then $NaBH_4$, MeOH, 78%; (b) i) allylchloroformate, DMAP, dichloromethane, ii) TFA, dichloromethane, 71%; (c) RCO_2H, EDC, DMAP, dichloromethane d) 1 N NaOH, THF, (50–62% for two steps, compounds **5**–**21**)

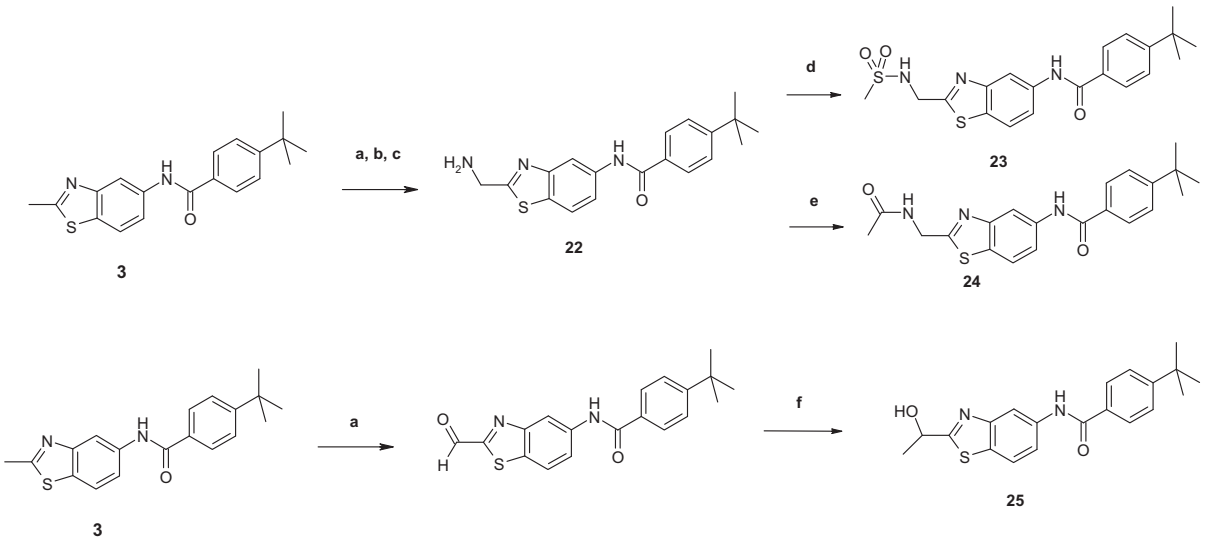

Scheme 2. *Reagents and conditions:*(a) SeO_2, Dioxane, 83%; (b) $NH_2OH.HCl$, KOAc, EtOH; (c) Zn, KOAc, AcOH, 48% from steps b–c; (d) MsCl, Et_3N, dichloromethane, 20%; (e) AcCl, Et_3N, dichloromethane, 75%; (f) MeMgBr, THF, 67%

Table 1
Potency of hydroxylated benzothiazole amides at human recombinant TRPV1

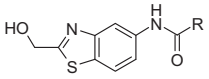

Compound	R	hIC_{50} (nM)[a]	Sol (μM)[b]	Human CLint (μL/ min/mg)	Compound	R	hIC_{50} (nM) [a]	Sol (μM) [b]	Human CLint (μL/min/ mg)
5	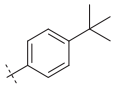	3.7	6	57	**14**	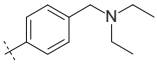	>10,000	5161	
6	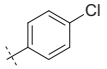	68.2	3	14	**15**	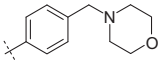	>10,000	419	13
7	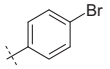	26.5	5		**16**	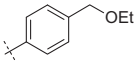	489.5	37	24
8	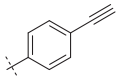	175.4	25		**17**	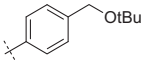	52.2	11	
9	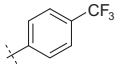	11.9			**18**	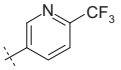	417.2	61	13
10	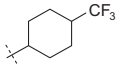	>10,000	77		**19**	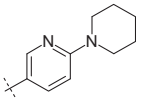	85.6	4	
11	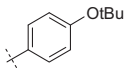	9.8	64	19	**20**	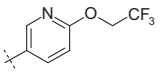	41.0	9	
12	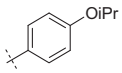	33.4	38	12	**21**	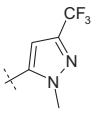	157.0	14	9
13	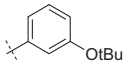	1072	181						

[a] Test compound induced inhibition of the increase in intracellular calcium in response to capsaicin addition in whole cells quantified in a Molecular Devices FLIPR IITM instrument imaging assay.
[b] Solubility of test compound in 0.1 M sodium phosphate buffer.

basic conditions (Scheme 4). Synthesis of reverse sulfonamide analog **32** required diazotization of aniline **4** and conversion to the corresponding sulfonyl chloride with sodium sulfite and copper sulfite in hydrochloric acid. Analog **33** was synthesized in

Table 2
Potency of derivatives with hydroxy replacements at human recombinant TRPV1

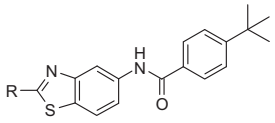

Compound	R	hIC_{50} (nM)	Compound	R	hIC_{50} (nM)
5	$-CH_2OH$	3.7	**24**	$-CH_2NHAc$	2415
22	$-CH_2NH_2$	987	**25**	–CH(Me)OH	223
23	CH_2NHSO_2Me	708			

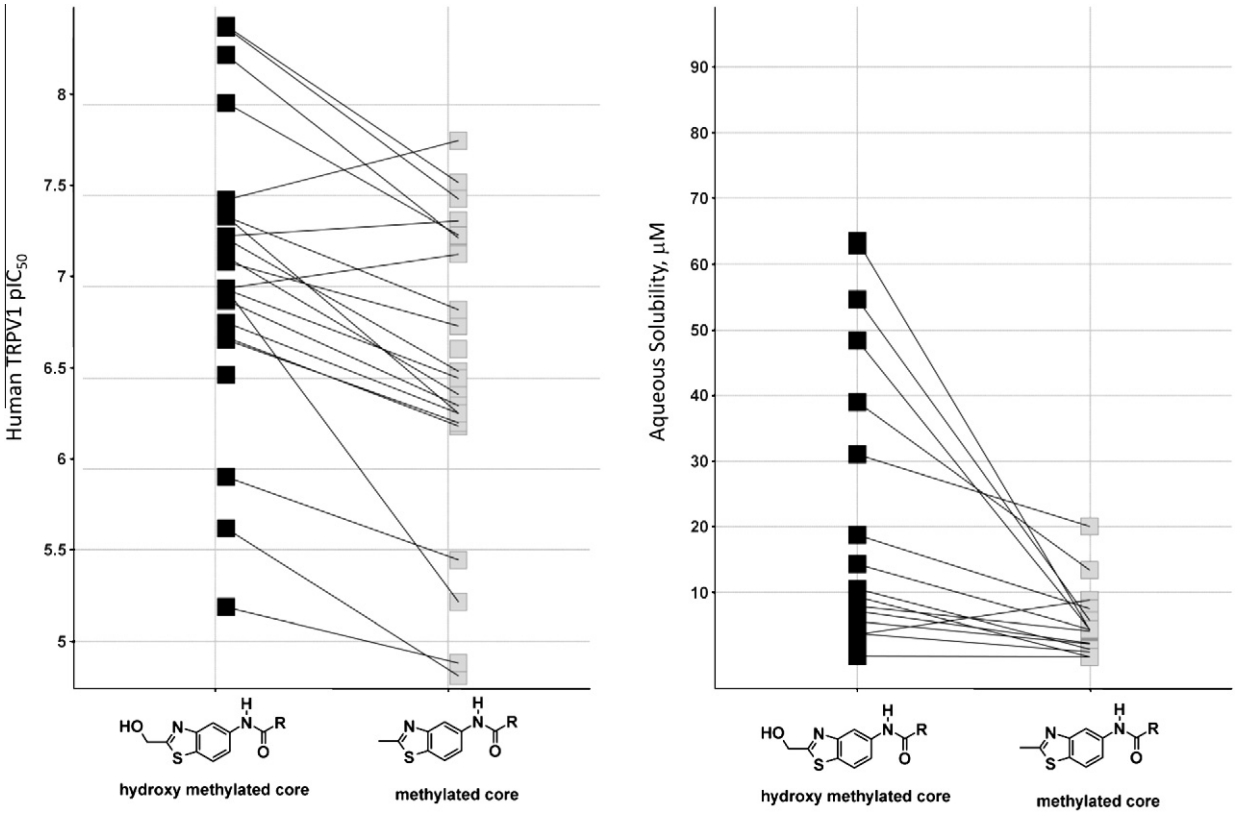

Figure 3. Matched pairs analysis for methyl to hydroxyl methyl transform on VR1 potency and aqueous solubility.

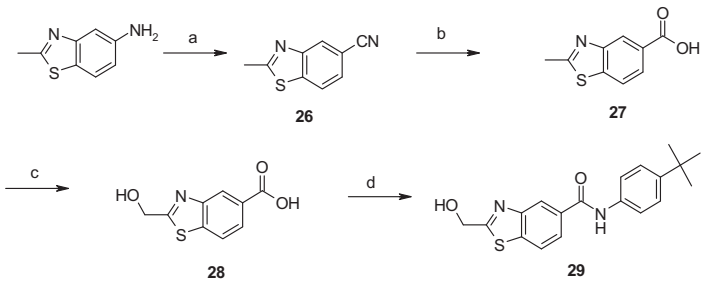

Scheme 3. *Reagents and conditions:*(a) i) $NaNO_2$, HCl, KI, acetone, water, ii) $Zn(CN)_2$, $Pd(PPh_3)_4$, dimethylformamide (b) HCl, 32% yield from (a) to (b); (c) i) SeO_2, dioxane, ii) $NaBH_4$, MeOH; (d) 4-*t*-butylaniline, EDC, DMAP, CH_2Cl_2, 22% from (c) to (d)

a similar fashion. Amine **34** was furnished by reductive amination of aniline **4** with 4-*tert*-butylbenzaldehyde followed by deprotection of the allylcarbonate protecting group.

Representative data is shown in Table 3 and demonstrates that replacement of the central amide with reverse amide, sulfonamide or reverse sulfomanide groups resulted in a dramatic decrease in

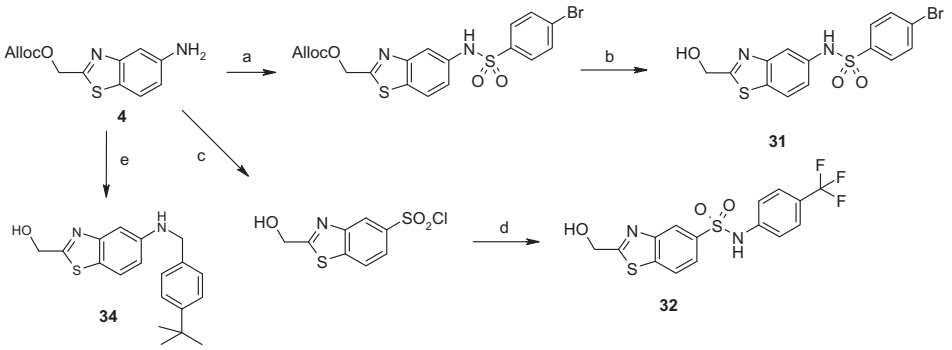

Scheme 4. *Reagents and conditions:*(a) $ArSO_2Cl$, $NaHCO_3$, THF; (b) NaOH, THF, 78% yield from (a) to (b); (c) i) HCl, $NaNO_2$, water, ii) Na_2SO_3, $CuSO_3$, HCl, water; (d) 4-trifluoromethylaniline, $NaHCO_3$, THF, 13% yield from (c) to (d). (e) i) 4-*tert*-butylbenzaldehyde, acetic acid:water 1:1, $NaBH(OAc)_3$, ii) NaOH, THF, 15%.

activity. By comparing amide **7** with sulfonamide **31**, amide **9** with reverse sulfonamide **32**, amide **5** with reverse amide **29** and amide **5** compared to aniline **34** it is clear that the original amide group is preferred for TRPV1 activity, possibly due to the defined direction of the hydrogen and carbonyl, that is, optimal for activity at the ion channel. Exploration of extended lypophilic groups, as highlighted by benzylic substituted **33** and phenethyl substituted amide **30** did show some indication of activity but physiochemical properties were suboptimal and it was felt that these modifications would not lead to productive areas for further exploration.

From work described so far, the hydroxyl methyl benzamide series was the most promising series for evaluation in rodent models of pain. However, despite advances in improving the solubility and metabolic stability of the series when evaluated in human and rat microsomes, rat in vivo clearance of these analogs was generally higher than expected as well as the measured clearance in vitro in rat hepatocytes (data not shown). Improvements in rat hepatic stability were required to generate compounds with an appropriate pharmokinetic profile to test in rodent models of pain. Biotransformation studies indicated that in vitro metabolism in rat hepatocytes (as well as human hepatocytes) occurred through amide hydrolysis, with the liberated aniline acetylated (Scheme 5).[11] Further experimental details can be found in ref. 11 and structures of the metabolites were confirmed by comparison with chemically synthesized standards. We suspected that the amide hydrolysis was in part responsible for the high clearance observed in rats and that a strategy was required to reduce amide hydrolysis.

We postulated that steric hinderence ortho to the amide group would decrease amide hydrolysis and hence decrease the clearance in vitro in rat hepatocytes, resulting in a favourable in vivo pharmokinetic profile. An *ortho*-methyl group on the benzamide showed a successful reduction in the measured clearance in rat hepatocytes as shown in Table 4. Compare the pairs of compounds **6** and **35**, **12** and **36** and **7** and **37** Furthermore, potency at the target was generally unaffected as was aqueous solubility. The resulting improvements in compound stability yielded compounds **35**, **36** and **37** with pharmacokinetic profiles suitable for exploration of compound effects in rodent inflammatory pain models. Of these three compounds, analog **37** was evaluated in two rodent models of pain.

Compound **37** has an affinty of 1 μM at rat VR1 when stimulated by capsaicin or protons, a bioavailability of 53% in rat and i.v. half life of 2.4 h. Evaluation in a rat capsaicin model of inflammatory pain[12] at a single dose experiment of 90 μmol/kg p.o. of **37**, gave a robust 72% block of paw withdrawal latency (Fig. 4). Likewise, evaluation in a rat carrageenan model of inflammatory pain[12] at a single dose experiment of 100 μmol/kg p.o. of **37**, gave a moderate but significant 35% reversal of the paw withdrawal latency. By comparison, the COX-2 inhibitor celecoxib in the same model also produced 35% reversal at the equivalent dose (data not shown). Interestingly, at the same dose no effect on core body temperature was observed. Previous reports have documented a rise in core body temperature during rodent experiments as well as in human clinical trials[13] and although we cannot rule out body

Table 3
Potency of amide linker replacements at human recombinant TRPV1

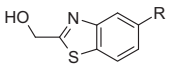

Compound	R	hIC_{50} (nM)	Compound	R	hIC_{50} (nM)
29	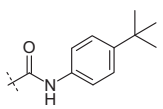	>10,000	**32**	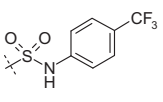	5575
30	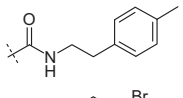	1605	**33**	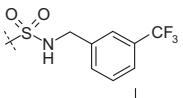	2871
31	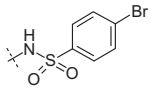	>10,000	**34**	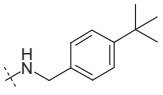	833

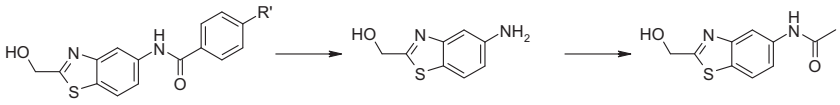

Scheme 5. Amide hydrolysis on incubation in vitro with rat hepatocytes.

Table 4

Effect of introducing a methyl group ortho to the amide 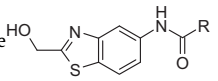

Compound	R	hIC_{50} (nM)	Rat hepatocytes (μL/min/10^6 cells)	Sol (μM)
6	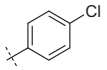	68.2	66	3
35	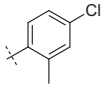	85.9	17	7
12	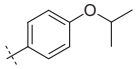	33.4	57	38
36	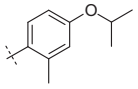	46.7	12	9
7	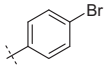	26.5	54	5
37	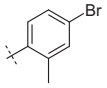	52.3	24	10

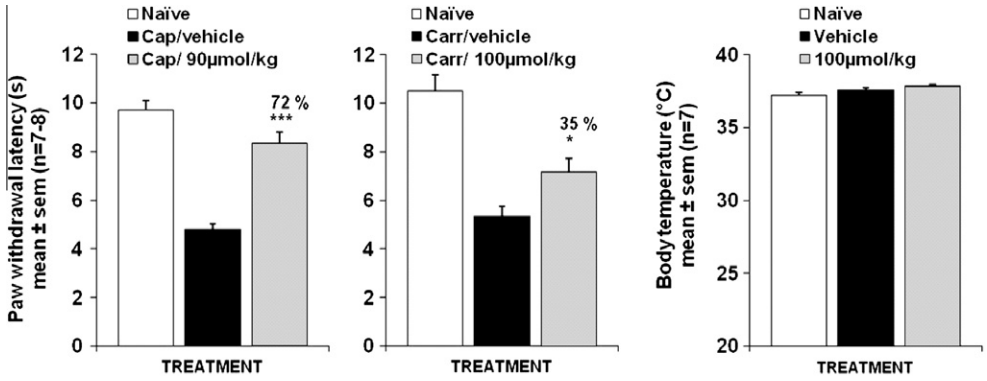

Figure 4. Effect of compound **37** in rat capsaicin model of inflammatory pain, effect in reversing thermal hyperalgesia in the carrageenan thermal hyperalgesia model and effect on core body temperature

temperature effects with **37** at higher doses, we do not observe body temperature effects at an efficacious dose.

Conclusion

Starting from a benzothiazole HTS hit we have systematically probed the key requirements for potent TRPV1 activity, while aiming to improve metabolic stability and aqueous solubility of the series. Although improvements in metabolic stability have been realized, improvements in aqueous solubility have been modest, highlighting a preference for TRPV1 antagonists to be reasonably lypophilic. From our studies, the hydroxymethylbenzimidazole series demonstrated the best overall profile with steric blocking of the amide group essential to reduce rat in vivo clearance. Compound **37** was active in a rat carrageenan model of inflammatory pain with no observed body temperature effects seen at an efficacious dose.

References and notes

1. (a) Caterina, M. J.; Schumacher, M. A.; Tominaga, M.; Rosen, T. A.; Levine, J. D.; Julius, D. *Nature* **1997**, *389*, 816; (b) García-Martínez, C.; Morenilla-Palao, C.; Planells-Cases, R.; Merino, J. M.; Ferrer-Montiel, A. *J. Biol. Chem.* **2000**, *275*, 32552; Birnbaumer, L.; Eda Yidirim, E.; Abramowitz, J. *Cell Calcium* **2003**, *33*, 419.
2. Patapoutian, A.; Peier, A. M.; Story, G. M.; Viswanath, V. *Nat. Rev. Neurosci.* **2003**, *4*, 529.
3. (a) Jordt, S. E.; Tominaga, M.; Julius, D. *Proc. Natl. Acad. Sci.* **2000**, *97*, 8134; (b) Welch, J. M.; Simon, S. A.; Reinhart, P. H. *Proc. Natl. Acad. Sci.* **2000**, *97*, 13889.
4. (a) Nagy, I.; Rang, H. P. *J. Neurosci.* **1999**, *19*, 10647; (b) Jung, J.; Lee, S.-Y.; Hwang, S. W.; Cho, H.; Shin, J.; Kang, Y.-S.; Kim, S.; Oh, U. *J. Biol. Chem.* **2002**, *277*, 44448; (c) Jordt, S.; Julius, D. *Cell* **2002**, *108*, 421.

5. (a) Gavva, N. R.; Klionsky, L.; Qu, Y.; Shi, L.; Tamir, R.; Edenson, S.; Zhang, T. J.; Viswanadhan, V. N.; Toth, A.; Pearce, L. V.; Vanderah, T. W.; Porreca, F.; Blumberg, P. M.; Lile, J.; Sun, Y.; Wild, K.; Louis, J.; Treanor, J. J. S. *J. Biol. Chem.* **2004**, *279*, 20283; (b) Takeuchi, K.; Murayama, N.; Toyooka, H.; Tominaga, M. *Proc. Natl. Acad. Sci.* **2003**, *100*, 8002.
6. (a) Chuang, H.; Prescott, E. D.; Kong, H.; Shields, S.; Jordt, S.; Basbaum, A.; Chao, M. V.; Julius, D. *Nature* **2001**, *411*, 957; (b) Premkumar, L. S.; Aherm, G. P. *Nature* **2000**, *408*, 985; (c) Numazaki, M.; Tominaga, T.; Toyooka, H.; Tominaga, M. D. *J. Biol. Chem.* **2002**, *277*, 13375; (d) Bhave, G.; Zhu, W.; Wang, H.; Brasier, D. J.; Oxford, G. S.; Gereau, R. W. *Neuron* **2002**, *35*, 721; (e) Olah, Z.; Karai, L.; Iadarola, M. J. *J. Biol. Chem.* **2002**, *277*, 35752; (f) Zhou, Y.; Li, G.; Zhao, Z. *J. Neurochem.* **2003**, *85*, 571; (g) Vulcu, S. D.; Rupp, J.; Wiwie, C.; Gillen, C.; Jostock, R.; Nawrath, H. *Pharmacology* **2003**, *69*, 38; (h) Chuang, H.; Prescott, E. D.; Kong, H.; Shields, S.; Jordt, S.; Basbaum, A. I.; Chao, M. V.; Julius, D. *Nature* **2001**, *411*, 957.
7. (a) Davis, J. B.; Gray, J.; Gunthorpe, M. J.; Hatcher, J. P.; Davey, P. T.; Overend, P.; Harries, M. H.; Latcham, J.; Clapham, C.; Atkinson, K.; Hughes, S. A.; Rance, K.; Grau, E.; Harper, A. J.; Pugh, P. L.; Rogers, D. C.; Bingham, S.; Randall, A.; Sheardown, S. A. *Nature* **2000**, *405*, 183; (b) Caterina, M. J.; Leffler, A.; Malmberg, A. B.; Martin, W. J.; Trafton, J.; Petersen-Zeitz, K. R.; Koltzenburg, M.; Basbaum, A. I.; Julius, D. *Science* **2000**, *288*, 306.
8. Walpole, C. S. J.; Bevan, S.; Bovermann, G.; Boelsterli, J. J.; Breckenridge, R.; Davies, J. W.; Hughes, G. A.; James, I.; Oberer, L.; Winter, J.; Wrigglesworth, R. *J. Med. Chem.* **1942**, *1994*, 37; (b) Walker, K. M.; Urban, L.; Medhurst, S. J.; Patel, S.; Panesar, M.; Fox, A. J.; McIntyre, P. *J. Pharmacol. Exp. Ther.* **2003**, *304*, 56.
9. (a) Walpole, C. S. J.; Wrigglesworth, R.; Bevan, S.; Campbell, E. A.; Dray, A.; James, I. F.; Perkins, M. N.; Reid, D. J.; Winter, J. *J. Med. Chem.* **1993**, *36*, 2362; (b) Walpole, C. S. J.; Wrigglesworth, R.; Bevan, S.; Campbell, E. A.; Dray, A.; James, I. F.; Masdin, K. J.; Perkins, M. N.; Reid, D. J.; Winter, J. *J. Med. Chem.* **1993**, *36*, 2373; (c) Walpole, C. S. J.; Wrigglesworth, R.; Bevan, S.; Campbell, E. A.; Dray, A.; James, I. F.; Masdin, K. J.; Perkins, M. N.; Reid, D. J.; Winter, J. *J. Med. Chem.* **1993**, *36*, 2381; (d) Wrigglesworth, R.; Walpole, C. S. J.; Bevan, S.; Campbell, E. A.; Dray, A.; Hughes, G. A.; James, I.; Masdin, K. J.; Winter, J. *J. Med. Chem.* **1996**, *39*, 4942; (e) Walpole, C. S. J.; Bevan, S.; Bloomfield, G.; Breckenridge, R.; James, I. F.; Ritchie, T.; Szallasi, A.; Winter, J.; Wrigglesworth, R. *J. Med. Chem.* **1996**, *39*, 2939; (f) Dray, A.; Bettaney, J.; Rueff, A.; Walpole, C.; Wrigglesworth, R. *Eur. J. Pharmacol.* **1990**, *181*, 289.
10. (a) Besidski, Y.; Brown, W.; Johnstone, S.; Labrecque, D.; Munro, A.; Rotticci, D.; Walpole, C.; Zemribo, R. WO 2004096784.; (b) Westaway, S. M.; Thompson, M.; Rami, H. K.; Stemp, G.; Trouw, L. S.; Mitchell, D. J.; Seal, J. T.; Medhurst, S. J.; Lappin, S. C.; Biggs, J.; Wright, J.; Arpino, S.; Jerman, J. C.; Cryan, J. E.; Holland, V.; Winborn, K. Y.; Coleman, T.; Stevens, A. J.; Davis, J. B.; Gunthorpe, M. J. *Bioorg. Med. Chem. Lett.* **2008**, *18*, 5609; (c) Duncton, M. A. J.; Ayala, L.; Kaub, C.; Janagani, S.; Edwards, W. T.; Orike, N.; Ramamoorthy, K.; Kincaid, J.; Kelly, M. G. *Tetrahedron Lett.* **2010**, *51*, 1009; (d) Kuramochi, T.; Hirabayashi, R.; Koganemaru, Y.; Munakata, R.; Yonezawa, K.; Kiso, T. WO 2007063925.
11. Bylund, J.; Petersson, C.; Lindgren, A.; Olofsson, S.; Czene, S. *Xenobiotica* **2012**, in press. http://dx.doi.org/10.3109/00498254.2012.708459.
12. Experiments were conducted in male Sprague–Dawley rats (125–200 g, Charles River., St Constant, Canada). Rats (groups of 7) were housed in a temperature controlled environment (22 ± 1.5 °C, 30–80% relative humidity, 12-h light/dark) and were acclimatized in the animal facility for at least 3 days prior to use. This study was conducted under a protocol that has been approved by AstraZeneca Animal Care Committee. The animals were kept and experiments were performed at our main site (AZRDM: AstraZeneca R&D Montreal) and has accreditation from CCAC (Canadian Council on Animal Care) and AAALAC (Association for the Assessment and Accreditation of Laboratory Animal Care) and approved by AZ GVC (AstraZeneca Global Veterinary Council) for study conduct. Experiments were performed during the light phase of the cycle. Animals had food (Harlan Teklad, Montreal, Canada) and water *ad libitum*. The number of animals used was the minimum necessary to achieve an 80% statistical power at a 30% reversal of hyperalgesia. In all experiments, naïve rats were used as controls. *Induction and assessment of the rat carrageenan model of inflammatory pain:* Under isoflurane anesthesia, inflammation was induced by the single administration of 100 μl of 1% carrageenan solution, Sigma) injected into the subcutaneous space of the plantar aspect of the left hind paw, in the center of the pads. All experiments were conducted 3 h after carrageenan administration.
    In order to assess the degree of heat hyperalgesia, the rats were placed individually in Plexiglas boxes on the glass surface (maintained at 30 °C) of the paw thermal stimulator system (IITC Life Science, Woodland Hills, USA, Model 390 Series 8), and allowed to acclimate for 30 min. A thermal stimulus, in the form of a radiant heat beam was focused onto the plantar surface of the affected paw. In each test session, rats were tested twice at approximately 5 min apart. Paw withdrawal latencies (PWLs) were calculated as the mean of the two values. An assay cut off was set at 20 s. *Induction and assessment of the rat capsaicin model of inflammatory pain:* Rats were gently placed in light restrainers with the left hind paw protruding. The left hind paw was immobilized and the needle was inserted intradermally (superficial layer) and laterally on the plantar aspect of the paw proximal to the heel. Capsaicin was injected at a dose 10 μg/5 μL. Rats were placed individually in Plexiglas boxes on the glass surface of the paw thermal stimulator system and tested 30 min for heat hyperalgesia as described above.
13. (a) Gavva, N. R. *Trends in Pharm. Sci.* **2008**, *29*, 550; (b) Tamayo, N.; Liao, H.; Stec, M. M.; Wang, X.; Chakrabarti, P.; Retz, D.; Doherty, E. M.; Surapaneni, S.; Tamir, R.; Bannon, A. W.; Gavva, N. R.; Norman, M. H. *J. Med. Chem.* **2008**, *51*, 2744.